Atmos. Chem. Phys. Discuss., doi:10.5194/acp-2017-77, 2017
Manuscript under review for journal Atmos. Chem. Phys.
Published: 31 January 2017

Atmospheric Chemistry and Physics Discussions

Formation of secondary organic aerosols from gas–phase emissions of heated cooking oils

Tengyu Liu[1], Zijun Li[2], ManNin Chan[2,3], and Chak K. Chan[1,*]

1. School of Energy and Environment, City University of Hong Kong, Hong Kong, China.
2. Earth System Science Programme, The Chinese University of Hong Kong, Hong Kong, China.
3. The Institute of Environment, Energy and Sustainability, The Chinese University of Hong Kong, Hong Kong, China

*Corresponding author:
Dr. Chak K. Chan
School of Energy and Environment, City University of Hong Kong
Tel: +852-34425593
Email: Chak.K.Chan@cityu.edu.hk

Atmos. Chem. Phys. Discuss., doi:10.5194/acp-2017-77, 2017
Manuscript under review for journal Atmos. Chem. Phys.
Published: 31 January 2017

Atmospheric Chemistry and Physics Discussions

Abstract

Cooking emissions can potentially contribute to secondary organic aerosol (SOA) but remain poorly understood. In this study, formation of SOA from gas-phase emissions of five heated vegetable oils (i.e. corn, canola, sunflower, peanut and olive oils) was investigated in a potential aerosol mass (PAM) chamber. Experiments were conducted at 19-20 ºC and 65-70% RH. The characterization instruments included a scanning mobility particle sizer (SMPS) and a high-resolution time-of-flight aerosol mass spectrometer (HR-TOF-AMS). The efficiency of SOA production, in ascending order, was peanut oil, olive oil, canola oil, corn oil and sunflower oil. The major SOA precursors from heated cooking oils were related to the content of mono-unsaturated fat and omega-6 fatty acids in cooking oils. The average production rate of SOA, after aging at an OH exposure of 1.7×10^{11} molecules cm^{-3} s, was 1.35±0.30 μg min^{-1}, three orders of magnitude lower compared with emission rates of fine particulate matter ($PM_{2.5}$) from heated cooking oils in previous studies. The mass spectra of cooking SOA highly resemble field-derived COA (cooking-related organic aerosol) in ambient air, with R^2 ranging from 0.74 to 0.88, suggesting that COA might not be entirely primary in origin. The average carbon oxidation state (OS_c) of SOA was -1.51 – -0.81, falling in the range between ambient hydrocarbon-like organic aerosol (HOA) and semi-volatile oxygenated organic aerosol (SV-OOA), indicating that SOA in these experiments was lightly oxidized.

Atmos. Chem. Phys. Discuss., doi:10.5194/acp-2017-77, 2017
Manuscript under review for journal Atmos. Chem. Phys.
Published: 31 January 2017

Atmospheric Chemistry and Physics Discussions

1. Introduction

Organic aerosol (OA) is an important component of atmospheric particulate matter (PM), which influences air quality, climate and human health (Hallquist et al., 2009). A significant fraction of OA is secondary organic aerosol (SOA) (Zhang et al., 2007), formed via the oxidation of volatile organic compounds (VOCs) (Hallquist et al., 2009). However, chemical transport models generally underestimate SOA levels due to the unclear sources and formation processes of SOA (de Gouw et al., 2005; Heald et al., 2005; Johnson et al., 2006; Volkamer et al., 2006). Recently, primary semi-volatile and intermediate-volatility organic compounds (SVOCs and IVOCs) that can come from the evaporation of primary organic aerosol (POA) were found to form substantial SOA (Robinson et al., 2007; Donahue et al., 2009). Therefore, any source of POA may be associated with the production of SOA.

Cooking-related organic aerosol (COA), thought to be primary in origin, contributed 10–34.6% of the total OA in urban areas (Allan et al., 2010; Sun et al., 2011; 2012; Ge et al., 2012; Mohr et al., 2012; Crippa et al., 2013; Lee et al., 2015). Lee et al. (2015) found that COA even dominated the contribution to POA at roadside sites in the commercial and shopping area of Mongkok in Hong Kong. Cooking may be a large source of SOA in urban areas, yet the formation of SOA from cooking remains poorly understood. Kaltsonoudis et al. (2016) observed that the oxygen to carbon ratio (O:C) of OA from meat charbroiling increased from 0.09 to 0.30 after a few hours of chemical aging. The aged aerosol mass spectra have similarities with ambient COA factors in two major Greek cities. Hayes et al. (2015) modeled that cooking emissions contributed

Atmos. Chem. Phys. Discuss., doi:10.5194/acp-2017-77, 2017
Manuscript under review for journal Atmos. Chem. Phys.
Published: 31 January 2017

Atmospheric Chemistry and Physics Discussions

19–35% of SOA mass in downtown Los Angeles during the California Research at the Nexus of Air Quality and Climate Change (CalNex) 2010 campaign. In their study, primary SVOCs and IVOCs from cooking emissions were modeled using the same parameters as those from vehicle exhaust, due to limited information about SOA formation from cooking (Hayes et al., 2015).

Heating cooking oils, a fundamental process of frying, was found to produce large amounts of fine particulate matter ($PM_{2.5}$) (Amouei Torkmahalleh et al, 2012; Gao et al., 2013) and VOCs (Katragadda et al., 2010; Klein et al., 2016a). The $PM_{2.5}$ emission rate for peanut, canola, corn and olive oils heated at 197 °C was shown to be as high as 54 mg min^{-1} (Amouei Torkmahalleh et al, 2012). Allan et al. (2010) found that cooking oils may contribute more to PM than the meat itself in urban areas of London and Manchester. The VOCs emitted from heated cooking oils were dominated by aldehydes (Klein et al., 2016a), which were suggested to be potential SOA precursors (Chacon-Madrid et al., 2010). Despite these previous efforts, there are still no available data regarding SOA formation from heated cooking oils.

The objective of this study is to characterize SOA formation from gas–phase emissions of heated cooking oils. The magnitude and composition of the SOA formed from gas–phase emissions of heated cooking oils were evaluated and have been discussed for the first time in this paper.

2. Materials and methods

2.1 PAM chamber

Atmos. Chem. Phys. Discuss., doi:10.5194/acp-2017-77, 2017
Manuscript under review for journal Atmos. Chem. Phys.
Published: 31 January 2017

SOA formation from gas–phase emissions of five different heated cooking oils was investigated in a potential aerosol mass (PAM) chamber, which has been described in detail elsewhere (Kang et al., 2007, 2011; Lambe et al., 2011, 2015). Briefly, a PAM chamber is a continuous flow stainless steel cylindrical reactor using high and controlled levels of oxidants to oxidize precursor gases to produce SOA. The volume is approximately 19 L (length 60 cm, diameter 20 cm). High OH exposures were produced through the photolysis of ozone irradiated by a UV lamp (λ = 254 nm) in the presence of water vapor. Ozone was produced by an ozone generator (1000BT-12, ENALY, Japan) via irradiation of pure O_2. The OH concentration was controlled by the flow rate of ozone in the PAM chamber, which was approximately 40 ppm prior to dilution. The total flow rate in the PAM chamber was set at 3 L min^{-1} by a mass flow controller, resulting in residence time of 380 s. The corresponding upper limit of OH exposure at these operating conditions was 1.7×10^{11} molecules cm^{-3} s, which is equivalent to 1.3 days of atmospheric oxidation, assuming an ambient OH concentration of 1.5×10^{6} molecules cm^{-3} (Mao et al., 2009). The upper limit of OH exposure was determined by measuring the decay of SO_2 (Model T100, TAPI Inc, USA), following previous procedures (Kang et al., 2007; Lambe et al., 2011). Before and after each experiment, the PAM reactor was cleaned by exposure to a high concentration of OH until the mass concentration of background particles was less than 5 μg m^{-3}.

The PAM chamber was designed with a large radius and a small surface-to-volume ratio to minimize wall effects. The transmission efficiency for particles at a mean mobility diameter (D_m) larger than 150 nm was greater than 80% (Lambe et al., 2011).

Atmos. Chem. Phys. Discuss., doi:10.5194/acp-2017-77, 2017
Manuscript under review for journal Atmos. Chem. Phys.
Published: 31 January 2017

Atmospheric Chemistry and Physics Discussions

The wall loss of particles was considered to be small, as the particles larger than 150 nm accounted for greater than 70% of the aerosol mass (Fig. S1 in the supporting information). Transmission efficiency of gases in the PAM chamber indicates that vapor wall losses in the PAM chamber are negligible (Lambe et al., 2011).

2.2 Experimental conditions

A schematic of the experimental setup is shown in Fig. 1. The tested vegetable oils, purchased from a local supermarket, included canola, corn, sunflower, peanut and olive oils. For each experiment, 30 mL vegetable oil was heated at approximately 220 ºC for 20 min in a 500 mL Pyrex bottle on an electric heating plate. Prior to introduction to the PAM chamber, particles from the heated oil emissions were removed using a Teflon filter. A 2 m Teflon tube was used as the transfer line to minimize wall loss of VOCs. After 10 min of heating, the UV lamp was turned on and the emissions were exposed to high OH levels for approximately one hour. Once the UV lamp was turned off, the PAM reactor was flushed continuously using pure N_2 and O_2 until the aerosol mass was below 3 μg m^{-3}. Then the experiment was repeated at another OH level. The RH and temperature of the PAM outflow were measured continuously (HMP 110, Vaisala Inc, Finland) and stabilized at 65-70% and 19-20 ºC, respectively. The adjustment of RH was achieved by passing the pure N_2 and O_2 through water bubblers. Blank experiments were conducted in the absence of cooking oils under similar conditions to quantify the amount of aerosols formed from matrix gas when exposed to different OH levels.

POA emitted from heated cooking oils was also characterized in this study. For each test, 30 mL vegetable oil was heated to 240 ºC for 2 min in a pan on an induction

Atmos. Chem. Phys. Discuss., doi:10.5194/acp-2017-77, 2017
Manuscript under review for journal Atmos. Chem. Phys.
Published: 31 January 2017

cooker. The emissions, after passing through a mixing chamber of 36 L, were introduced to the PAM chamber by a Dekati diluter (Dekati Ltd, Finland) at a flow rate of 0.15 L min^{-1}, achieving a final dilution ratio of approximately 160. No ozone was introduced to the PAM chamber during measurement, and the UV lamp was off. Temperature and RH were similar to those of the SOA formation experiments.

A scanning mobility particle sizer (SMPS, TSI Incorporated, USA, classifier model 3082, CPC model 3775) was used to measure particle number concentrations and size distributions. Particle size ranged from 15 nm to 661 nm. An aerosol density of 1.4 g cm^{-3} was assumed to estimate the SOA mass from the particle volume concentration (Zhang et al., 2005). For the SOA formation experiments, the contribution from background organic aerosols was subtracted from the total organic aerosols. The maximum concentration of background organic aerosols was 8.4 μg m^{-3}, almost negligible compared with the dozens to several hundreds of μg m^{-3} of SOA formed in this study. The organic aerosol composition was characterized by a high-resolution time-of-flight aerosol mass spectrometer (HR-TOF-AMS, abbreviated as AMS hereafter, Aerodyne Research Incorporated, USA) (DeCarlo et al., 2006). A diffusion dryer was connected to the sampling line to remove water. The instrument was operated in the high sensitivity V-mode and high resolution W-mode alternating every one minute. The toolkit Squirrel 1.57I and Pika 1.16I were used to analyze the AMS data. The molar ratios of hydrogen to carbon (H:C) and oxygen to carbon (O:C) were determined with the improved-ambient method (Canagaratna et al., 2015). The ionization efficiency of AMS was calibrated using 300 nm ammonium nitrate particles.

Atmos. Chem. Phys. Discuss., doi:10.5194/acp-2017-77, 2017
Manuscript under review for journal Atmos. Chem. Phys.
Published: 31 January 2017

Atmospheric Chemistry and Physics Discussions

145 The particle-free matrix air, obtained by passing the air through a HEPA filter, was
146 measured for at least 20 min before each experiment to determine the signals from
147 major gases. The collection efficiency (CE) was corrected by comparing AMS mass
148 concentrations to concurrent SMPS mass concentrations, following the methods of
149 Gordon et al. (2014) and Liu et al., (2015).

150 **2.3 SOA production rate**

151 The SOA production rate (PR) was expressed as micrograms (μg) of SOA produced
152 per minute (min), calculated using the following equation, similar to calculation of
153 emissions rates of primary particles from cooking (Klein et al., 2016a):

154 $$PR = [SOA] \times DR \times F \quad (1)$$

155 where [SOA] is the SOA concentration in μg m^{-3}; DR is the dilution ratio and F is the
156 flow rate in m^3 min^{-1} of the carrier gas. All gas-phase emissions from heated cooking
157 oils were assumed to be transported into the PAM chamber.

158 Emission rates are commonly used to normalize PM emissions from cooking
159 activities (Amouei Torkmahalleh et al, 2012; Gao et al., 2013; Klein et al., 2016a, b).
160 Here, the adoption of SOA PR, similar to emission rates, facilitates the normalization
161 of SOA production from cooking and direct comparison of the amount of primary
162 emitted and secondary formed particles. Though SOA yields were not determined due
163 to the lack of VOC concentrations, we believe that SOA PR is a useful metric for the
164 estimation of SOA production from cooking and can be used for comparison among
165 different studies.

166 ## 3. Results and discussion

Atmos. Chem. Phys. Discuss., doi:10.5194/acp-2017-77, 2017
Manuscript under review for journal Atmos. Chem. Phys.
Published: 31 January 2017

Atmospheric Chemistry and Physics Discussions

3.1 SOA formation

In Fig. 2, we plot the time series of RH, ozone and organic aerosol concentrations during the aging of gas–phase emissions from heated peanut oil. As described above, the ozone concentration prior to dilution was stable at approximately 40 ppm. The pulse of RH was caused by disconnection of the introduction line when changing the Teflon filter. During the initial 10 min of heating, the mass concentration of organics was close to the detection limit of the instrument, indicating that POA emissions were thoroughly removed by the Teflon filter. Immediately after oxidation was initiated by turning on the UV lamp, substantial SOA was formed, and its concentration stabilized after about 20 min. The SOA concentration subsequently reported is the average for the steady period.

Fig. 3 shows SOA concentration as a function of OH exposure and photochemical age in days during the aging of gas–phase emissions from different heated cooking oils. The OH exposure ranged from 2.7×10^{10} molecules cm^{-3} s to 1.7×10^{11} molecules cm^{-3} s, corresponding to 0.2–1.3 days of photochemical age, assuming 24 h average ambient OH concentrations of 1.5×10^{6} molecules cm^{-3} (Mao et al., 2009). For all experiments, the SOA concentration almost linearly increased from 41–107 μg m^{-3} to 320–565 μg m^{-3} as OH exposure increased. This linear increase has also been observed from vehicle exhaust at a similar range of OH exposures (Tkacik et al., 2014). Typically, VOCs are oxidized through functionalization reactions to produce less volatile organics that readily condense to form SOA. Upon further oxidation, fragmentation reactions and cleavage of carbon bonds can occur and form more volatile products that reduce SOA

Atmos. Chem. Phys. Discuss., doi:10.5194/acp-2017-77, 2017
Manuscript under review for journal Atmos. Chem. Phys.
Published: 31 January 2017

levels (Kroll et al., 2009). In this study, functionalization reactions dominated SOA formation as reflected by the increase of SOA concentrations shown in Fig. 3.

The slope of the fitted straight line to the SOA data was calculated to estimate the efficiency of different cooking oils in producing SOA (Table 1). The efficiency of SOA production, in ascending order, was peanut oil, olive oil, canola oil, corn oil and sunflower oil. The slope of sunflower oil was 3.82×10^{-15} μg molecules^{-1} s^{-1}, more than two times that of peanut oil. The different slopes might be related to the emission rate and composition of VOCs from various cooking oils. Table 1 presents the type of fat content of the different cooking oils. Unsaturated fat accounts for 75%-88% of the total fat content. A multivariate linear regression was used to relate the SOA production efficiency to the fat content of cooking oils. The intercept was set to zero. The resulting equation was $Y = 2.62\times10^{-17}X_1 + 4.71\times10^{-17}X_2$, where Y is the SOA production efficiency (μg molecules^{-1} s^{-1}); X_1 and X_2 represent the content of mono-unsaturated fat (%) and omega-6 fatty acid (%) in cooking oil, respectively. The SOA production efficiency was strongly correlated ($R^2 = 0.97$, $p<0.05$) with the content of mono-unsaturated fat and omega-6 fatty acids. This indicated that the major SOA precursors from heated cooking oils were related to the content of mono-unsaturated fat and omega-6 fatty acids in cooking oils. Moreover, omega-6 fatty acids dominated the contribution to SOA production. Omega-6 fatty acids are a family of poly-unsaturated fatty acids that have in common a final carbon-carbon double bond in the n-6 position, counting from the methyl end (Simopoulos, 2002). The peroxyl radical reactions of

Atmos. Chem. Phys. Discuss., doi:10.5194/acp-2017-77, 2017
Manuscript under review for journal Atmos. Chem. Phys.
Published: 31 January 2017

omega-6 fatty acids might emit long-chain aldehydes (Gardner, 1989), which have been suggested as potential SOA precursors (Chacon-Madrid et al., 2010).

The average SOA PR from gas–phase emissions of the five cooking oils at an OH exposure of 1.7×10^{11} molecules cm^{-3} s was calculated to be 1.35±0.30 μg min^{-1}. Amouei Torkmahalleh et al. (2012) found that primary $PM_{2.5}$ emission rates for peanut, canola, corn and olive oils heated at 197 °C ranged from 3.7 mg min^{-1} to 54 mg min^{-1}. He et al. (2004) reported a $PM_{2.5}$ emission rate for frying in vegetable oils of 2.68±2.18 mg^{-} min^{-} ^{1}. The SOA PR determined in this study was negligible compared with primary $PM_{2.5}$ emission rates for heated cooking oils and frying in vegetable oils. However, our results may underestimate SOA production from cooking under real-world conditions. First, recent studies have demonstrated that the oxidation of IVOCs and SVOCs evaporated from POA could produce significant SOA (Donahue et al., 2006; Jimenez et al., 2009). In this study, POA from heated cooking oils was filtered. Second, emissions of SOA precursors will be enhanced when cooking food compared with heating cooking oils alone. For instance, long-chain aldehyde emissions from frying processes can be 10 times those of heated oil (Klein et al., 2016a). Large amounts of monoterpenes will be emitted when frying vegetables or cooking with herbs and black pepper (Klein et al., 2016a, b). These enhanced emitted precursors may significantly enhance SOA production. Finally, laboratory and tunnel studies indicate that SOA production from typical precursors and vehicle exhaust peak at OH exposures higher than 5.0×10^{11} molecules cm^{-3} s (Tkacik et al., 2014; Lambe et al., 2015). The relatively lower OH

Atmos. Chem. Phys. Discuss., doi:10.5194/acp-2017-77, 2017
Manuscript under review for journal Atmos. Chem. Phys.
Published: 31 January 2017

Atmospheric Chemistry and Physics Discussions

exposures in this study compared with typical conditions in the atmosphere may lead to the underestimation of cooking SOA.

3.2 Mass spectra of POA and SOA

Fig. 4 shows high-resolution mass spectra of POA and SOA at an OH exposure of 2.7×10^{10} molecules cm^{-3} s from heated canola oil. Other oils have similar mass spectra, as reflected in the good correlations shown in Table 2. The mass concentration of POA was approximately 35 μg m^{-3} for canola oil. The prominent peaks in POA from canola oil were m/z 41 and 55, followed by m/z 29 and 43. The m/z 41, 43 and 55 were dominated by $C_3H_5^+$, $C_3H_7^+$ and $C_4H_7^+$ ion series, consistent with the previous observation by Allan et al. (2010). The m/z 29 was instead dominated by ion CHO^+, which can be used as a tracer for organic compounds with alcohol and carbonyl functional groups, as a result of thermal decomposition of the oils (Lee et al., 2012). For the SOA mass spectra, the dominating peaks were m/z 28 and 29, followed by m/z 43 and 44. The m/z 28, 29, 43 and 44 were dominated by CO^+, CHO^+, $C_2H_3O^+$ and CO_2^+, respectively. For all cooking oils, the mass fractions of m/z 28 and 44 in SOA were higher, while the mass fractions of m/z 55 and 57 in SOA were lower than those of the corresponding POA. The increase of mass fractions of the oxygen-containing ions in SOA mass spectra indicated the formation of oxidized organic aerosols.

The correlation coefficients (R^2) between POA and SOA unit mass resolution (UMR) spectra of heated oil and COA resolved by positive matrix factorization (PMF) analysis (Lee et al., 2015) were calculated and summarized in Table 2 to evaluate their similarities. The POA mass spectra between different cooking oils exhibited strong

Atmos. Chem. Phys. Discuss., doi:10.5194/acp-2017-77, 2017
Manuscript under review for journal Atmos. Chem. Phys.
Published: 31 January 2017

Atmospheric Chemistry and Physics Discussions

253 correlations (R^2>0.97) and agreed well with the ambient COA factor obtained at
254 roadside sites in the commercial and shopping area of Mongkok in Hong Kong (Lee et
255 al., 2015). The SOA mass spectra between different cooking oils displayed good
256 correlations (R^2>0.94), suggesting a high degree of similarity. The mass spectra of
257 cooking SOA also greatly resemble POA and field-derived COA in ambient air, with
258 R^2 ranging from 0.74 to 0.88. This similarity between the cooking SOA and ambient
259 COA suggests that the COA resolved based on ambient data may be a convolution of
260 POA and SOA, even though vegetable oil may not be the oil commonly used in
261 commercial kitchens. Kaltsonoudis et al. (2016) also observed that the ambient COA
262 factor in two major Greek cities in spring and summer strongly resembled the aged
263 SOA from meat charbroiling in a smog chamber.

264 Fragments derived from the AMS data have been extensively used to explore the
265 bulk compositions and properties of ambient organic aerosols (Zhang et al., 2005; Ng
266 et al., 2010; Heald et al., 2010). Here, we use the approach of Ng et al. (2010) by
267 plotting the fractions of the total organic signal at m/z 43 (f_{43}) vs. m/z 44 (f_{44}). The m/z
268 43 signal is abundant in $C_3H_7^+$ and $C_2H_3O^+$ ions, indicating fresh, less oxidized organic
269 aerosols. The m/z 44 signal, usually dominated by CO_2^+ and formed from the thermal
270 decarboxylation of organic acids, is an indicator of highly oxygenated organic aerosols
271 (Ng et al., 2010).

272 In Fig. 5, we plot f_{43} vs. f_{44} of cooking SOA and SOA data from gasoline (Presto
273 et al., 2014; Liu et al., 2015) and diesel (Presto et al., 2014) vehicle exhaust measured
274 in a smog chamber, together with the triangle defined by Ng et al. (2010) based on the

Atmos. Chem. Phys. Discuss., doi:10.5194/acp-2017-77, 2017
Manuscript under review for journal Atmos. Chem. Phys.
Published: 31 January 2017

Atmospheric Chemistry and Physics Discussions

analysis of ambient AMS data. The ambient low-volatility oxygenated OA (LV-OOA) and semi-volatile OOA (SV-OOA) factors fall in the upper and lower regions of the triangle, respectively. Ng et al. (2010) proposed that aging would converge the f_{43} and f_{44} toward the triangle apex (f_{43} = 0.02, f_{44} = 0.30). In this study, the f_{43} and f_{44} ranged from 0.06 to 0.10 and from 0.05 to 0.07, respectively; they mainly lie in the lower portion of the SV-OOA region. As shown in Fig. 5, SOA from gasoline and diesel vehicle exhaust at a similar range of OH exposures had f_{44} values of 0.11–0.12. Compared with vehicle exhaust, SOA formed from gas-phase emissions of heated cooking oils was less oxidized. The potential SOA precursors from heated cooking oils might be long-chain aldehydes, which are less volatile than SOA precursors such as aromatics and long-chain alkanes from vehicle exhaust. A single polar moiety of first-generation products from long-chain aldehydes will have low enough volatility to condense, while more volatile aromatics and long-chain alkanes require more functionalization to form SOA (Donahue et al., 2012). Therefore, SOA formed from heated cooking oils was less oxidized. For each cooking oil, there was little change in f_{44} and a slight increase in f_{43} as OH exposure increased. The increased SOA mass may facilitate the partitioning of more volatile organics, leading to a slight increase in f_{43} and little change in f_{44}. This is consistent with the observation of previous studies that the f_{44} of SOA from aromatics and monoterpenes varied little and that f_{43} increased slightly for SOA mass loadings higher than 100 μg m^{-3} (Ng et al., 2010; Kang et al., 2011).

3.3 Chemical composition of SOA

Atmos. Chem. Phys. Discuss., doi:10.5194/acp-2017-77, 2017
Manuscript under review for journal Atmos. Chem. Phys.
Published: 31 January 2017

Atmospheric Chemistry and Physics Discussions

297 The O:C ratio and the estimated average carbon oxidation state (OS_c) ($OSc \approx 2\times O:C - H:C$) (Kroll et al., 2011) can be used to evaluate the degree of oxidation of organic
298 aerosols. Fig. 6 shows the evolution of O:C ratios and OS_c of SOA from heated cooking
299 oils as a function of OH exposure, together with the POA data. The O:C ratios and OS_c
300 of POA were in the range of 0.14–0.23 and -1.61 – -1.44, respectively, comparable to
301 those of POA from meat charbroiling (Kaltsonoudis et al., 2016). As shown in Fig. 6,
302 for each cooking oil, the O:C and OS_c of SOA displayed similar trends, initially
303 decreasing rapidly and then increasing slowly or leveling off (for canola oil only). In
304 this study, the increased SOA mass loadings led to the rapid decrease of the oxidation
305 degree when the OH exposure increased from 2.7×10^{10} molecules cm^{-3} s to 6.4×10^{10}
306 molecules cm^{-3} s. As OH exposure and the resulting OA mass loadings further increase,
307 even less oxidized and more volatile organics partition into the particle phase and thus
308 decrease the oxidation degree (Donahue et al., 2006). The difference in O:C for
309 different cooking oils at the same OH exposure may be attributed to the differences in
310 gas-phase SOA precursors. In general, the O:C ratios of SOA formed from gas–phase
311 emissions of heated cooking oils ranged from 0.24 to 0.46 at OH exposures of 2.7×10^{10}
312 – 1.7×10^{11} molecules cm^{-3} s. The OS_c of cooking SOA was -1.51 – -0.81, falling in the
313 range between ambient hydrocarbon-like organic aerosol (HOA, OS_c = -1.69) and SV-
314 OOA (OS_c = -0.57) corrected by the improved-ambient method (Canagaratna et al.,
315 2015). As suggested by Canagaratna et al. (2015), the OS_c is more robust than the f_{43}/f_{44}
316 relationship for evaluating the oxidation degree of organic aerosols, as the former has
317 been estimated based on the full spectra.

Atmos. Chem. Phys. Discuss., doi:10.5194/acp-2017-77, 2017
Manuscript under review for journal Atmos. Chem. Phys.
Published: 31 January 2017

Atmospheric Chemistry and Physics Discussions

In Fig. S2 we plot the H:C and O:C molar ratios of POA and SOA from heated cooking oils on a Van Krevelen diagram. The cooking data fell along a line with a slope of approximately 0, suggesting the chemistry of SOA formation in this study was alcohol/peroxide formation (Heald et al., 2010; Ng et al., 2011). This slope is different from ambient OA data of -0.8 determined by the improved-ambient method (Heald et al., 2010). It is also different from vehicle exhaust data with slopes ranging from -0.59 to -0.36 (Presto et al., 2014; Liu et al., 2015).

4. Conclusions

Formation of SOA from gas-phase emissions of heated cooking oils was investigated in a PAM chamber at OH exposures of 2.7×10^{10} molecules cm^{-3} s to 1.7×10^{11} molecules cm^{-3} s. The OS_c and f_{43}/f_{44} relationship indicated that the SOA formed was lightly oxidized. The mass spectra of SOA highly resembled POA from heated cooking oils and COA factors in ambient air. These similarities indicated that ambient COA factors identified by AMS could contain cooking SOA. The major SOA precursors from heated cooking oils were related to the content of mono-unsaturated fat and omega-6 fatty acids in cooking oils. Considering that animal fats such as pork and chicken fat are also abundant in mono-unsaturated fat and omega-6 fatty acids, gas-phase emissions from cooking animal fat can be as efficient as vegetable oils in producing SOA. It is important to note that the reported SOA data only related to gas-phase emissions from heated cooking oils. The large amounts of POA emitted from cooking oils may also form SOA after photochemical aging. More work is needed to investigate SOA formation from emissions of cooking oils and food. In addition, gas-phase SOA

Atmos. Chem. Phys. Discuss., doi:10.5194/acp-2017-77, 2017
Manuscript under review for journal Atmos. Chem. Phys.
Published: 31 January 2017

Atmospheric Chemistry and Physics Discussions

precursors were not characterized and therefore provided limited information on SOA yields from cooking; we recommend that future work validate our results and perform similar experiments, with gas-phase emissions measured.

Acknowledgments

The work described in this paper was partially sponsored by Project No. 41675117, supported by the National Natural Science Foundation of China, and was partially supported by the Shenzhen Research Institute, City University of Hong Kong. Li, Z. and Chan, M. N. are supported by a Direct Grant for Research (4053159), The Chinese University of Hong Kong.

Atmos. Chem. Phys. Discuss., doi:10.5194/acp-2017-77, 2017
Manuscript under review for journal Atmos. Chem. Phys.
Published: 31 January 2017

Atmospheric Chemistry and Physics Discussions

References

Allan, J. D., Williams, P. I., Morgan, W. T., Martin, C. L., Flynn, M. J., Lee, J., Nemitz, E., Phillips, G. J., Gallagher, M. W., and Coe, H.: Contributions from transport, solid fuel burning and cooking to primary organic aerosols in two UK cities, Atmos. Chem. Phys., 10, 647-668, doi:10.5194/acp-10-647-2010, 2010.

Amouei Torkmahalleh, M., Goldasteh, I., Zhao, Y., Udochu, N. M., Rossner, A., Hopke, P. K., and Ferro, A. R.: PM2.5 and ultrafine particles emitted during heating of commercial cooking oils, Indoor Air, 22, 483-491, doi:10.1111/j.1600-0668.2012.00783.x, 2012.

Canagaratna, M. R., Jimenez, J. L., Kroll, J. H., Chen, Q., Kessler, S. H., Massoli, P., Hildebrandt Ruiz, L., Fortner, E., Williams, L. R., Wilson, K. R., Surratt, J. D., Donahue, N. M., Jayne, J. T., and Worsnop, D. R.: Elemental ratio measurements of organic compounds using aerosol mass spectrometry: characterization, improved calibration, and implications, Atmos. Chem. Phys., 15, 253-272, doi:10.5194/acp-15-253-2015, 2015.

Chacon-Madrid, H. J., Presto, A. A., and Donahue, N. M.: Functionalization vs. fragmentation: n-aldehyde oxidation mechanisms and secondary organic aerosol formation, Phys. Chem. Chem. Phys, 12, 13975-13982, doi:10.1039/C0CP00200C, 2010.

Crippa, M., DeCarlo, P. F., Slowik, J. G., Mohr, C., Heringa, M. F., Chirico, R., Poulain, L., Freutel, F., Sciare, J., Cozic, J., Di Marco, C. F., Elsasser, M., Nicolas, J. B., Marchand, N., Abidi, E., Wiedensohler, A., Drewnick, F., Schneider, J., Borrmann, S., Nemitz, E., Zimmermann, R., Jaffrezo, J. L., Prévôt, A. S. H., and Baltensperger, U.: Wintertime aerosol chemical composition and source apportionment of the organic fraction in the metropolitan area of Paris, Atmos. Chem. Phys., 13, 961-981, doi:10.5194/acp-13-961-2013, 2013.

de Gouw, J. A., Middlebrook, A. M., Warneke, C., Goldan, P. D., Kuster, W. C., Roberts, J. M., Fehsenfeld, F. C., Worsnop, D. R., Canagaratna, M. R., Pszenny, A. A. P., Keene, W. C., Marchewka, M., Bertman, S. B., and Bates, T. S.: Budget of organic carbon in a polluted atmosphere: Results from the New England Air Quality Study in 2002, J. Geophys. Res.-Atmos., 110, D16305, doi:10.1029/2004JD005623, 2005.

DeCarlo, P. F., Kimmel, J. R., Trimborn, A., Northway, M. J., Jayne, J. T., Aiken, A. C., Gonin, M., Fuhrer, K., Horvath, T., Docherty, K. S., Worsnop, D. R., and Jimenez, J. L.: Field-Deployable, High-Resolution, Time-of-Flight Aerosol Mass Spectrometer, Anal. Chem., 78, 8281-8289, doi:10.1021/ac061249n, 2006.

Donahue, N. M., Robinson, A. L., Stanier, C. O., and Pandis, S. N.: Coupled Partitioning, Dilution, and Chemical Aging of Semivolatile Organics, Environ. Sci. Technol., 40, 2635-2643, doi:10.1021/es052297c, 2006.

Donahue, N. M., Robinson, A. L., and Pandis, S. N.: Atmospheric organic particulate matter: From smoke to secondary organic aerosol, Atmos. Environ., 43, 94-106, doi:10.1016/j.atmosenv.2008.09.055, 2009.

393 Donahue, N. M., Kroll, J. H., Pandis, S. N., and Robinson, A. L.: A two-dimensional
394 volatility basis set – Part 2: Diagnostics of organic-aerosol evolution, Atmos. Chem.
395 Phys., 12, 615-634, doi:10.5194/acp-12-615-2012, 2012.
396 Gao, J., Cao, C. S., Wang, L., Song, T. H., Zhou, X., Yang, J., and Zhang, X.: Determination
397 of Size-Dependent Source Emission Rate of Cooking-Generated Aerosol Particles at
398 the Oil-Heating Stage in an Experimental Kitchen, Aerosol Air Qual. Res., 13, 488-
399 496, doi:10.4209/aaqr.2012.09.0238, 2013.
400 Gardner, H. W.: Oxygen radical chemistry of polyunsaturated fatty acids, Free Radical Biol.
401 Med., 7, 65-86, doi:10.1016/0891-5849(89)90102-0, 1989.
402 Ge, X., Setyan, A., Sun, Y., and Zhang, Q.: Primary and secondary organic aerosols in
403 Fresno, California during wintertime: Results from high resolution aerosol mass
404 spectrometry, J. Geophys. Res.-Atmos., 117, D19301, doi:10.1029/2012JD018026,
405 2012.
406 Gordon, T. D., Presto, A. A., May, A. A., Nguyen, N. T., Lipsky, E. M., Donahue, N. M.,
407 Gutierrez, A., Zhang, M., Maddox, C., Rieger, P., Chattopadhyay, S., Maldonado, H.,
408 Maricq, M. M., and Robinson, A. L.: Secondary organic aerosol formation exceeds
409 primary particulate matter emissions for light-duty gasoline vehicles, Atmos. Chem.
410 Phys., 14, 4661-4678, doi:10.5194/acp-14-4661-2014, 2014.
411 Hallquist, M., Wenger, J. C., Baltensperger, U., Rudich, Y., Simpson, D., Claeys, M.,
412 Dommen, J., Donahue, N. M., George, C., Goldstein, A. H., Hamilton, J. F.,
413 Herrmann, H., Hoffmann, T., Iinuma, Y., Jang, M., Jenkin, M. E., Jimenez, J. L.,
414 Kiendler-Scharr, A., Maenhaut, W., McFiggans, G., Mentel, T. F., Monod, A.,
415 Prévôt, A. S. H., Seinfeld, J. H., Surratt, J. D., Szmigielski, R., and Wildt, J.: The
416 formation, properties and impact of secondary organic aerosol: current and emerging
417 issues, Atmos. Chem. Phys., 9, 5155-5236, doi:10.5194/acp-9-5155-2009, 2009.
418 Hayes, P. L., Carlton, A. G., Baker, K. R., Ahmadov, R., Washenfelder, R. A., Alvarez, S.,
419 Rappenglück, B., Gilman, J. B., Kuster, W. C., de Gouw, J. A., Zotter, P., Prévôt, A.
420 S. H., Szidat, S., Kleindienst, T. E., Offenberg, J. H., Ma, P. K., and Jimenez, J. L.:
421 Modeling the formation and aging of secondary organic aerosols in Los Angeles
422 during CalNex 2010, Atmos. Chem. Phys., 15, 5773-5801, doi:10.5194/acp-15-5773-
423 2015, 2015.
424 He, C., Morawska, L., Hitchins, J., and Gilbert, D.: Contribution from indoor sources to
425 particle number and mass concentrations in residential houses, Atmos. Environ., 38,
426 3405-3415, doi:10.1016/j.atmosenv.2004.03.027, 2004.
427 Heald, C. L., Jacob, D. J., Park, R. J., Russell, L. M., Huebert, B. J., Seinfeld, J. H., Liao, H.,
428 and Weber, R. J.: A large organic aerosol source in the free troposphere missing from
429 current models, Geophys. Res. Lett., 32, L18809, doi:10.1029/2005GL023831, 2005.
430 Heald, C. L., Kroll, J. H., Jimenez, J. L., Docherty, K. S., DeCarlo, P. F., Aiken, A. C., Chen,
431 Q., Martin, S. T., Farmer, D. K., and Artaxo, P.: A simplified description of the
432 evolution of organic aerosol composition in the atmosphere, Geophys. Res. Lett., 37,
433 L08803, doi:10.1029/2010gl042737, 2010.
434 Jimenez, J. L., Canagaratna, M. R., Donahue, N. M., Prevot, A. S. H., Zhang, Q., Kroll, J. H.,
435 DeCarlo, P. F., Allan, J. D., Coe, H., Ng, N. L., Aiken, A. C., Docherty, K. S.,
436 Ulbrich, I. M., Grieshop, A. P., Robinson, A. L., Duplissy, J., Smith, J. D., Wilson, K.

437 R., Lanz, V. A., Hueglin, C., Sun, Y. L., Tian, J., Laaksonen, A., Raatikainen, T.,
438 Rautiainen, J., Vaattovaara, P., Ehn, M., Kulmala, M., Tomlinson, J. M., Collins, D.
439 R., Cubison, M. J., E., Dunlea, J., Huffman, J. A., Onasch, T. B., Alfarra, M. R.,
440 Williams, P. I., Bower, K., Kondo, Y., Schneider, J., Drewnick, F., Borrmann, S.,
441 Weimer, S., Demerjian, K., Salcedo, D., Cottrell, L., Griffin, R., Takami, A.,
442 Miyoshi, T., Hatakeyama, S., Shimono, A., Sun, J. Y., Zhang, Y. M., Dzepina, K.,
443 Kimmel, J. R., Sueper, D., Jayne, J. T., Herndon, S. C., Trimborn, A. M., Williams,
444 L. R., Wood, E. C., Middlebrook, A. M., Kolb, C. E., Baltensperger, U., and
445 Worsnop, D. R.: Evolution of Organic Aerosols in the Atmosphere, Science, 326,
446 1525-1529, doi:10.1126/science.1180353, 2009.
447 Johnson, D., Utembe, S. R., Jenkin, M. E., Derwent, R. G., Hayman, G. D., Alfarra, M. R.,
448 Coe, H., and McFiggans, G.: Simulating regional scale secondary organic aerosol
449 formation during the TORCH 2003 campaign in the southern UK, Atmos. Chem.
450 Phys., 6, 403-418, doi:10.5194/acp-6-403-2006, 2006.
451 Kaltsonoudis, C., Kostenidou, E., Louvaris, E., Psichoudaki, M., Tsiligiannis, E., Florou, K.,
452 Liangou, A., and Pandis, S. N.: Characterization of fresh and aged organic aerosol
453 emissions from meat charbroiling, Atmos. Chem. Phys. Discuss., 2016, 1-27,
454 doi:10.5194/acp-2016-979, 2016.
455 Kang, E., Root, M. J., Toohey, D. W., and Brune, W. H.: Introducing the concept of Potential
456 Aerosol Mass (PAM), Atmos. Chem. Phys., 7, 5727-5744, doi:10.5194/acp-7-5727-
457 2007, 2007.
458 Kang, E., Toohey, D. W., and Brune, W. H.: Dependence of SOA oxidation on organic
459 aerosol mass concentration and OH exposure: experimental PAM chamber studies,
460 Atmos. Chem. Phys., 11, 1837-1852, doi:10.5194/acp-11-1837-2011, 2011.
461 Katragadda, H. R., Fullana, A., Sidhu, S., and Carbonell-Barrachina, Á. A.: Emissions of
462 volatile aldehydes from heated cooking oils, Food Chem., 120, 59-65,
463 doi:10.1016/j.foodchem.2009.09.070, 2010.
464 Klein, F., Platt, S. M., Farren, N. J., Detournay, A., Bruns, E. A., Bozzetti, C., Daellenbach,
465 K. R., Kilic, D., Kumar, N. K., Pieber, S. M., Slowik, J. G., Temime-Roussel, B.,
466 Marchand, N., Hamilton, J. F., Baltensperger, U., Prévôt, A. S. H., and El Haddad, I.:
467 Characterization of Gas-Phase Organics Using Proton Transfer Reaction Time-of-
468 Flight Mass Spectrometry: Cooking Emissions, Environ. Sci. Technol.,
469 doi:10.1021/acs.est.5b04618, 2016.
470 Kroll, J. H., Smith, J. D., Che, D. L., Kessler, S. H., Worsnop, D. R., and Wilson, K. R.:
471 Measurement of fragmentation and functionalization pathways in the heterogeneous
472 oxidation of oxidized organic aerosol, Phys. Chem. Chem. Phys., 11, 8005-8014,
473 doi:10.1039/B905289E, 2009.
474 Kroll, J. H., Donahue, N. M., Jimenez, J. L., Kessler, S. H., Canagaratna, M. R., Wilson, K.
475 R., Altieri, K. E., Mazzoleni, L. R., Wozniak, A. S., Bluhm, H., Mysak, E. R., Smith,
476 J. D., Kolb, C. E., and Worsnop, D. R.: Carbon oxidation state as a metric for
477 describing the chemistry of atmospheric organic aerosol, Nat. Chem., 3, 133-139,
478 2011.
479 Lambe, A. T., Ahern, A. T., Williams, L. R., Slowik, J. G., Wong, J. P. S., Abbatt, J. P. D.,
480 Brune, W. H., Ng, N. L., Wright, J. P., Croasdale, D. R., Worsnop, D. R., Davidovits,

P., and Onasch, T. B.: Characterization of aerosol photooxidation flow reactors: heterogeneous oxidation, secondary organic aerosol formation and cloud condensation nuclei activity measurements, Atmos. Meas. Tech., 4, 445-461, doi:10.5194/amt-4-445-2011, 2011.

Lambe, A. T., Chhabra, P. S., Onasch, T. B., Brune, W. H., Hunter, J. F., Kroll, J. H., Cummings, M. J., Brogan, J. F., Parmar, Y., Worsnop, D. R., Kolb, C. E., and Davidovits, P.: Effect of oxidant concentration, exposure time, and seed particles on secondary organic aerosol chemical composition and yield, Atmos. Chem. Phys., 15, 3063-3075, doi:10.5194/acp-15-3063-2015, 2015.

Lee, A. K. Y., Hayden, K. L., Herckes, P., Leaitch, W. R., Liggio, J., Macdonald, A. M., and Abbatt, J. P. D.: Characterization of aerosol and cloud water at a mountain site during WACS 2010: secondary organic aerosol formation through oxidative cloud processing, Atmos. Chem. Phys., 12, 7103-7116, doi:10.5194/acp-12-7103-2012, 2012.

Lee, B. P., Li, Y. J., Yu, J. Z., Louie, P. K. K., and Chan, C. K.: Characteristics of submicron particulate matter at the urban roadside in downtown Hong Kong—Overview of 4 months of continuous high-resolution aerosol mass spectrometer measurements, J. Geophys. Res.-Atmos., 120, JD023311, doi:10.1002/2015JD023311, 2015.

Liu, T., Wang, X., Deng, W., Hu, Q., Ding, X., Zhang, Y., He, Q., Zhang, Z., Lü, S., Bi, X., Chen, J., and Yu, J.: Secondary organic aerosol formation from photochemical aging of light-duty gasoline vehicle exhausts in a smog chamber, Atmos. Chem. Phys., 15, 9049-9062, doi:10.5194/acp-15-9049-2015, 2015.

Mao, J., Ren, X., Brune, W. H., Olson, J. R., Crawford, J. H., Fried, A., Huey, L. G., Cohen, R. C., Heikes, B., Singh, H. B., Blake, D. R., Sachse, G. W., Diskin, G. S., Hall, S. R., and Shetter, R. E.: Airborne measurement of OH reactivity during INTEX-B, Atmos. Chem. Phys., 9, 163-173, doi:10.5194/acp-9-163-2009, 2009.

Ng, N. L., Canagaratna, M. R., Zhang, Q., Jimenez, J. L., Tian, J., Ulbrich, I. M., Kroll, J. H., Docherty, K. S., Chhabra, P. S., Bahreini, R., Murphy, S. M., Seinfeld, J. H., Hildebrandt, L., Donahue, N. M., DeCarlo, P. F., Lanz, V. A., Prévôt, A. S. H., Dinar, E., Rudich, Y., and Worsnop, D. R.: Organic aerosol components observed in Northern Hemispheric datasets from Aerosol Mass Spectrometry, Atmos. Chem. Phys., 10, 4625-4641, doi:10.5194/acp-10-4625-2010, 2010.

Ng, N. L., Canagaratna, M. R., Jimenez, J. L., Chhabra, P. S., Seinfeld, J. H., and Worsnop, D. R.: Changes in organic aerosol composition with aging inferred from aerosol mass spectra, Atmos. Chem. Phys., 11, 6465-6474, doi:10.5194/acp-11-6465-2011, 2011.

Presto, A. A., Gordon, T. D., and Robinson, A. L.: Primary to secondary organic aerosol: evolution of organic emissions from mobile combustion sources, Atmos. Chem. Phys., 14, 5015-5036, doi:10.5194/acp-14-5015-2014, 2014.

Robinson, A. L., Donahue, N. M., Shrivastava, M. K., Weitkamp, E. A., Sage, A. M., Grieshop, A. P., Lane, T. E., Pierce, J. R., and Pandis, S. N.: Rethinking Organic Aerosols: Semivolatile Emissions and Photochemical Aging, Science, 315, 1259-1262, doi:10.1126/science.1133061, 2007.

523 Simopoulos, A. P.: The importance of the ratio of omega-6/omega-3 essential fatty acids,
524 Biomedicine & Pharmacotherapy, 56, 365-379, doi:10.1016/S0753-3322(02)00253-6,
525 2002.
526 Sun, Y. L., Zhang, Q., Schwab, J. J., Demerjian, K. L., Chen, W. N., Bae, M. S., Hung, H.
527 M., Hogrefe, O., Frank, B., Rattigan, O. V., and Lin, Y. C.: Characterization of the
528 sources and processes of organic and inorganic aerosols in New York city with a
529 high-resolution time-of-flight aerosol mass apectrometer, Atmos. Chem. Phys., 11,
530 1581-1602, doi:10.5194/acp-11-1581-2011, 2011.
531 Sun, Y. L., Zhang, Q., Schwab, J. J., Chen, W. N., Bae, M. S., Hung, H. M., Lin, Y. C., Ng,
532 N. L., Jayne, J., Massoli, P., Williams, L. R., and Demerjian, K. L.: Characterization
533 of near-highway submicron aerosols in New York City with a high-resolution aerosol
534 mass spectrometer, Atmos. Chem. Phys., 12, 2215-2227, doi:10.5194/acp-12-2215-
535 2012, 2012.
536 Tkacik, D. S., Lambe, A. T., Jathar, S., Li, X., Presto, A. A., Zhao, Y. L., Blake, D.,
537 Meinardi, S., Jayne, J. T., Croteau, P. L., and Robinson, A. L.: Secondary Organic
538 Aerosol Formation from in-Use Motor Vehicle Emissions Using a Potential Aerosol
539 Mass Reactor, Environ. Sci. Technol., 48, 11235-11242, doi:10.1021/es502239v,
540 2014.
541 Volkamer, R., Jimenez, J. L., San Martini, F., Dzepina, K., Zhang, Q., Salcedo, D., Molina, L.
542 T., Worsnop, D. R., and Molina, M. J.: Secondary organic aerosol formation from
543 anthropogenic air pollution: Rapid and higher than expected, Geophys. Res. Lett., 33,
544 L17811, doi:10.1029/2006gl026899, 2006.
545 Zhang, Q., Worsnop, D. R., Canagaratna, M. R., and Jimenez, J. L.: Hydrocarbon-like and
546 oxygenated organic aerosols in Pittsburgh: insights into sources and processes of
547 organic aerosols, Atmos. Chem. Phys., 5, 3289-3311, doi:10.5194/acp-5-3289-2005,
548 2005.
549 Zhang, Q., Jimenez, J. L., Canagaratna, M. R., Allan, J. D., Coe, H., Ulbrich, I., Alfarra, M.
550 R., Takami, A., Middlebrook, A. M., Sun, Y. L., Dzepina, K., Dunlea, E., Docherty,
551 K., DeCarlo, P. F., Salcedo, D., Onasch, T., Jayne, J. T., Miyoshi, T., Shimono, A.,
552 Hatakeyama, S., Takegawa, N., Kondo, Y., Schneider, J., Drewnick, F., Borrmann,
553 S., Weimer, S., Demerjian, K., Williams, P., Bower, K., Bahreini, R., Cottrell, L.,
554 Griffin, R. J., Rautiainen, J., Sun, J. Y., Zhang, Y. M., and Worsnop, D. R.: Ubiquity
555 and dominance of oxygenated species in organic aerosols in anthropogenically-
556 influenced Northern Hemisphere midlatitudes, Geophys. Res. Lett., 34, L13801,
557 doi:10.1029/2007gl029979, 2007.

Atmos. Chem. Phys. Discuss., doi:10.5194/acp-2017-77, 2017
Manuscript under review for journal Atmos. Chem. Phys.
Published: 31 January 2017

Atmospheric Chemistry and Physics Discussions

558 **Table 1.** SOA production efficiency and type of fat content (%) [a] of different cooking
559 oils.

	Slope [b] μg molecules^{-1} s^{-1}	Saturated (%)	Mono-unsaturated (%)	Poly-unsaturated (%)		Others (%)
				Omega-6	Omega-3	
sunflower	3.82×10^{-15}	10	19	64	0	7
corn	3.31×10^{-15}	12	24	56	1	7
canola	2.68×10^{-15}	7	59	20	9	5
olive	2.55×10^{-15}	13	71	8	1	7
peanut	1.7×10^{-15}	16	44	31	0	9

560 [a] The type of fat content of cooking oils was derived from skillsyouneed.com.
561 [b] SOA production efficiency was presented as the slope of the fitted straight line to the
562 SOA concentration vs OH exposure.
563
564

Atmos. Chem. Phys. Discuss., doi:10.5194/acp-2017-77, 2017
Manuscript under review for journal Atmos. Chem. Phys.
Published: 31 January 2017

Atmospheric Chemistry and Physics Discussions

565 **Table 2.** Correlation coefficients (R^2) between POA and SOA UMR mass spectra and
566 ambient COA resolved by PMF.

	CA P[a]	CN P	SR P	PT P	OE P	CA S	CN S	SR S	PT S	OE S	COA[b]
CA P	1.00	0.99	1.00	0.98	0.97	0.85	0.87	0.91	0.93	0.94	0.96
CN P	0.99	1.00	0.99	0.99	0.99	0.89	0.90	0.94	0.96	0.96	0.95
SR P	1.00	0.99	1.00	0.98	0.97	0.85	0.87	0.91	0.93	0.94	0.96
PT P	0.98	0.99	0.98	1.00	0.98	0.83	0.85	0.90	0.93	0.93	0.96
OE P	0.97	0.99	0.97	0.98	1.00	0.86	0.88	0.93	0.95	0.96	0.94
CA S	0.85	0.89	0.85	0.83	0.86	1.00	0.95	0.98	0.96	0.94	0.74
CN S	0.87	0.90	0.87	0.85	0.88	0.95	1.00	0.95	0.96	0.96	0.77
SR S	0.91	0.94	0.91	0.90	0.93	0.98	0.95	1.00	0.99	0.97	0.83
PT S	0.93	0.96	0.93	0.93	0.95	0.96	0.96	0.99	1.00	0.99	0.87
OE S	0.94	0.96	0.94	0.93	0.96	0.94	0.96	0.97	0.99	1.00	0.88

567 [a] CA, CN, SR, PT and OE refer to canola, corn, sunflower, peanut and olive oil.
568 [b] Lee et al. (2015).
569

Atmos. Chem. Phys. Discuss., doi:10.5194/acp-2017-77, 2017
Manuscript under review for journal Atmos. Chem. Phys.
Published: 31 January 2017

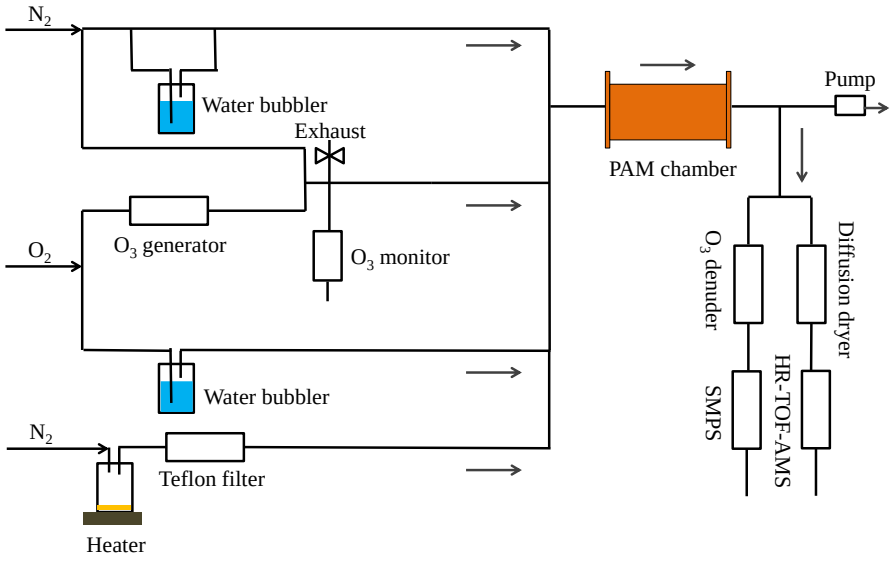

570

571 **Fig. 1.** Schematic of the experimental setup.

572

Atmos. Chem. Phys. Discuss., doi:10.5194/acp-2017-77, 2017
Manuscript under review for journal Atmos. Chem. Phys.
Published: 31 January 2017

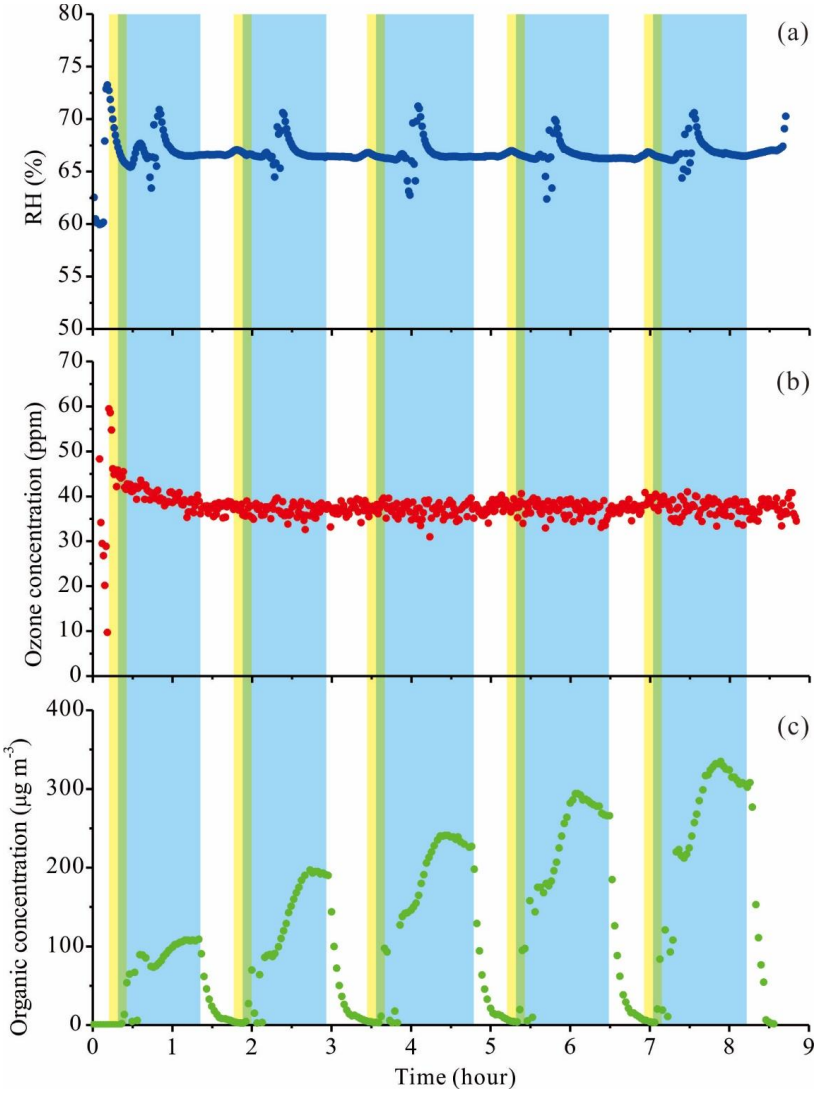

573

574 **Fig. 2.** Time series of (a) relative humidity (RH), (b) ozone and (c) organic
575 concentrations during the aging of gas–phase emissions from heated peanut oil. The
576 yellow and light blue regions represent the heating oil and OH exposure period,
577 respectively. The green region is the overlap between heating oil and OH exposure
578 period.

579

Atmos. Chem. Phys. Discuss., doi:10.5194/acp-2017-77, 2017
Manuscript under review for journal Atmos. Chem. Phys.
Published: 31 January 2017

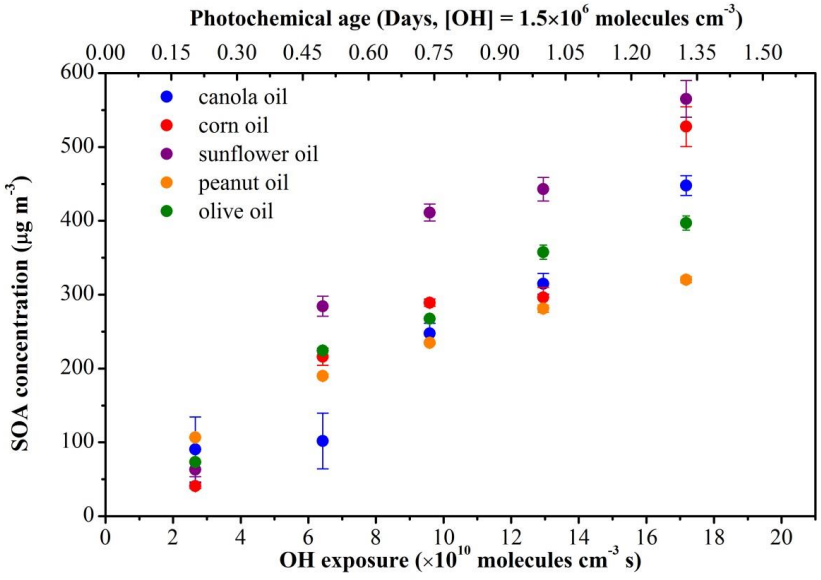

580

581 **Fig. 3.** SOA concentration vs. OH exposure and photochemical age in days (at [OH] =

582 1.5×10^6 molecules cm^{-3}) during the aging of gas–phase emissions from different heated

583 cooking oils. Error bars represent the standard deviation (1σ).

584

Atmos. Chem. Phys. Discuss., doi:10.5194/acp-2017-77, 2017
Manuscript under review for journal Atmos. Chem. Phys.
Published: 31 January 2017

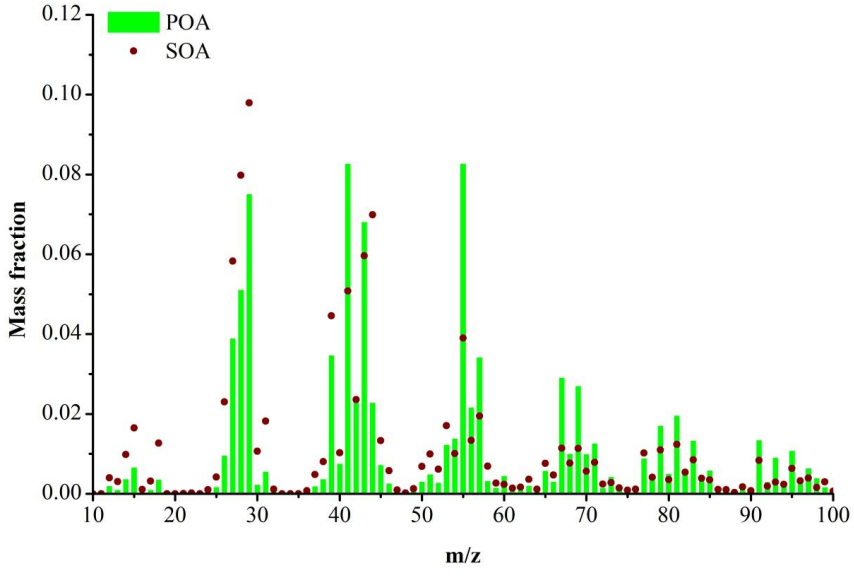

585

586 **Fig. 4.** Mass spectra of POA and SOA at an OH exposure of 2.7×10^{10} molecules cm^{-3} s

587 from heated canola oil.

588

Atmos. Chem. Phys. Discuss., doi:10.5194/acp-2017-77, 2017
Manuscript under review for journal Atmos. Chem. Phys.
Published: 31 January 2017

Atmospheric Chemistry and Physics Discussions

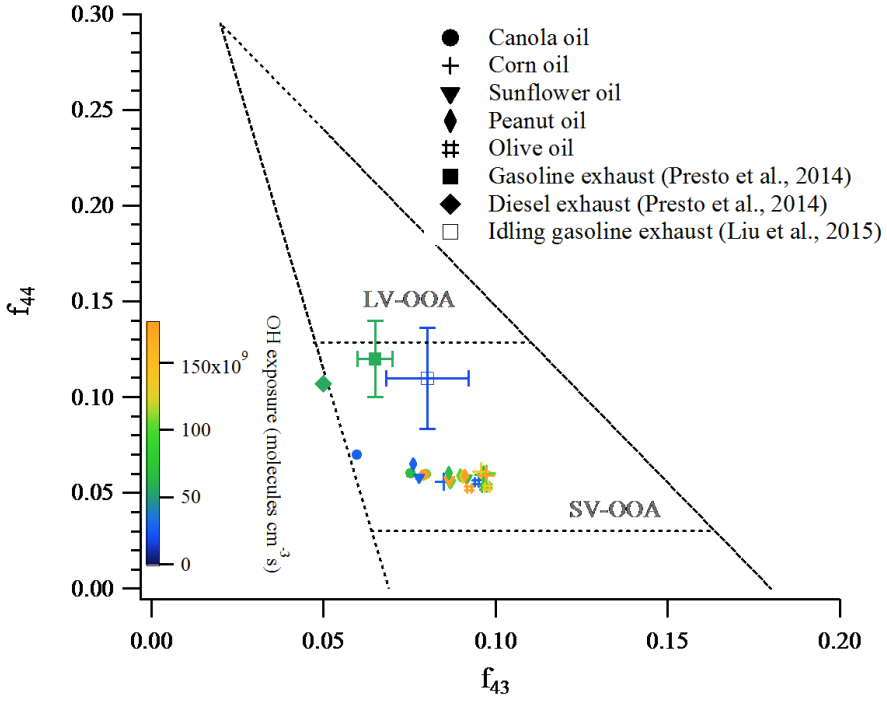

589

590 **Fig. 5.** Fractions of total organic signal at m/z 43 (f_{43}) vs. m/z (f_{44}) from SOA data in
591 this work together with the triangle plot of Ng et al. (2010). SOA data from gasoline
592 (Presto et al., 2014; Liu et al., 2015) and diesel (Presto et al., 2014) vehicle exhaust
593 measured in smog chamber studies are shown. Data from this work and the literature
594 are colored according to OH exposure. Ambient SV–OOA and LV–OOA regions are
595 adapted from Ng et al. (2010).

596

Atmos. Chem. Phys. Discuss., doi:10.5194/acp-2017-77, 2017
Manuscript under review for journal Atmos. Chem. Phys.
Published: 31 January 2017

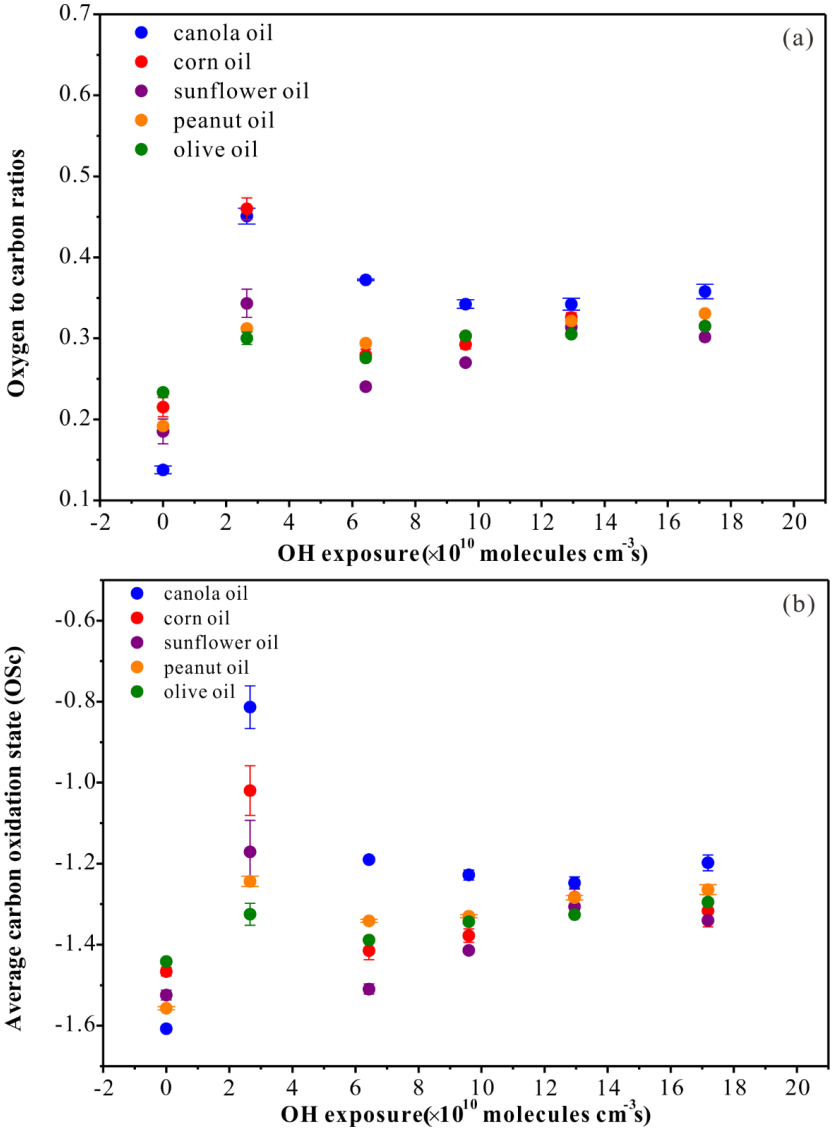

Fig. 6. Evolution of (a) oxygen to carbon (O:C) molar ratios and (b) average carbon oxidation state (OS_c) as a function of OH exposure during the aging of gas–phase emissions from heated different cooking oils, with error bars indicating standard error. Data at [OH] = 0 represent POA from cooking oils.